Effects of lymphocyte profile on development of EBV-induced lymphoma subtypes in humanized mice

Eun Kyung Lee[a,b,1], Eun Hye Joo[a,b,1], Kyung-A Song[a,b,1], Bongkum Choi[b,c], Miyoung Kim[b,c], Seok-Hyung Kim[a,b,d], Sung Joo Kim[a,b,c,2], and Myung-Soo Kang[a,b,2]

[a]Samsung Advanced Institute for Health Sciences and Technology, Samsung Medical Center and Sungkyunkwan University, Seoul 06351, Korea; [b]Samsung Biomedical Research Institute, Seoul 06351, Korea; [c]Department of Transplantation Surgery, Samsung Medical Center and Sungkyunkwan University School of Medicine, Seoul 06351, Korea; and [d]Department of Pathology, Samsung Medical Center and Sungkyunkwan University School of Medicine, Seoul 06351, Korea

Edited by Elliott Kieff, Harvard Medical School and Brigham and Women's Hospital, Boston, MA, and approved September 10, 2015 (received for review April 19, 2014)

Epstein-Barr virus (EBV) infection causes both Hodgkin's lymphoma (HL) and non-Hodgkin's lymphoma (NHL). The present study reveals that EBV-induced HL and NHL are intriguingly associated with a repopulated immune cell profile in humanized mice. Newborn immunodeficient NSG mice were engrafted with human cord blood CD34$^+$ hematopoietic stem cells (HSCs) for a 8- or 15-wk reconstitution period (denoted ^{8w}hN and ^{15w}hN, respectively), resulting in human B-cell and T-cell predominance in peripheral blood cells, respectively. Further, novel humanized mice were established via engraftment of hCD34$^+$ HSCs together with nonautologous fetal liver-derived mesenchymal stem cells (MSCs) or MSCs expressing an active notch ligand *DLK1*, resulting in mice skewed with human B or T cells, respectively. After EBV infection, whereas NHL developed more frequently in B-cell–predominant humanized mice, HL was seen in T-cell–predominant mice (P = 0.0013). Whereas human splenocytes from NHL-bearing mice were positive for EBV-associated NHL markers (hBCL2$^+$, hCD20$^+$, hKi67$^+$, hCD20$^+$/EBNA1$^+$, and EBER$^+$) but negative for HL markers (LMP1$^-$, EBNA2$^-$, and hCD30$^-$), most HL-like tumors were characterized by the presence of malignant Hodgkin's Reed–Sternberg (HRS)-like cells, lacunar RS (hCD30$^+$, hCD15$^+$, IgJ$^-$, EBER$^+$/hCD30$^+$, EBNA1$^+$/hCD30$^+$, LMP$^+$/EBNA2$^-$, hCD68$^+$, hBCL2$^-$, hCD20$^{-/weak,}$ Phospho STAT6$^+$), and mummified RS cells. This study reveals that immune cell composition plays an important role in the development of EBV-induced B-cell lymphoma.

Epstein–Barr virus | humanized mice | Non-Hodgkin's lymphoma | Hodgkin's lymphoma | Reed–Sternberg cell

Epstein Barr virus (EBV) infects human B lymphocytes and epithelial cells in >90% of the human population (1, 2). EBV infection is widely associated with the development of diverse human disorders that include Hodgkin's lymphoma (HL) and non-Hodgkin's lymphomas (NHL), including diffused large B-cell lymphoma (DLBCL), follicular B-cell lymphoma (FBCL), endemic Burkitt's lymphoma (BL), and hemophagocytic lymphohistiocytosis (HLH) (3).

HL is a malignant lymphoid neoplasm most prevalent in adolescents and young adults (4–6). Hodgkin/Reed–Sternberg (HRS) cells are the sole malignant cells of HL. HRS cells are characterized by CD30$^+$/CD15$^+$/BCL6$^-$/CD20$^{+/-}$ markers and appear large and multinucleated owing to multiple nuclear divisions without cytokinesis. Although HRS cells are malignant in the body, surrounding inflammatory cells greatly outnumber them. These reactive nonmalignant inflammatory cells, including lymphocytes, histiocytes, eosinophils, fibroblasts, neutrophils, and plasma cells, compose the vast majority of the tumor mass. The presence of HRS cells in the context of this inflammatory cellular background is a critical hallmark of the HL diagnosis (4). Approximately 50% of HL cases are EBV-associated (EBVaHL) (7–11). EBV-positive HRS cells express EBV latent membrane protein (LMP) 1 (LMP1), LMP2A, LMP2B, and EBV nuclear antigen (EBNA) 1 (EBNA1), but lack EBNA2 (latency II marker) (12). LMP1 is consistently expressed in all EBV-associated cases of classical HL (13, 14). LMP1 mimics activated CD40 receptors, induces NF-κB, and allows cells to become malignant while escaping apoptosis (15).

The etiologic role of EBV in numerous disorders has been studied in humanized mouse models in diverse experimental conditions. Humanized mouse models recapitulate key characteristics of EBV infection-associated disease pathogenesis (16–24). Different settings have given rise to quite distinct phenotypes, including B-cell type NHL (DLBCL, FBCL, and unspecified B-cell lymphomas), natural killer/T cell lymphoma (NKTCL), nonmalignant lymphoproliferative disorder (LPD), extremely rare HL, HLH, and arthritis (16–24). Despite considerable efforts (16–24), EBVaHL has not been properly produced in the humanized mouse setting model, owing to inappropriate animal models and a lack of in-depth analyses. After an initial report of infected humanized mice, HRS-like cells appeared to be extremely rare in the spleens of infected humanized mice; however, the findings were inconclusive (18). Here we report direct evidence of EBVaHL or HL-like neoplasms in multiple humanized mice in which T cells were predominant over B cells. Our study demonstrates that EBV-infected humanized mice display additional EBV-associated pathogenesis, including DLBCL and hemophagocytic lymphohistiocytosis (16, 17).

Results

NHL in B-Cell–Predominant ^{8w}hN-EBV Mice. In the first experimental trial, 13 newborn NSG mice were engrafted with hCD34$^+$ HSC for 8 wk (denoted by ^{8w}hN), after which components of the human immune system (HIS) (e.g., hCD45, hCD3, hCD19) were

Significance

The mechanism of how Epstein-Barr virus (EBV) contributes to the development of two distinct lymphomas remains unknown. Intriguingly, EBV-associated Hodgkin's lymphoma was seen exclusively in mice with activated T-cell conditions, whereas EBV-associated non-Hodgkin's lymphoma was developed in mice with suppressed T-cell conditions, in which immature B cells were predominant at the time of EBV infection. This distinct association provides new insight into the pathogenesis of specific types of EBV-induced lymphomas.

Author contributions: E.K.L., S.J.K., and M.-S.K. designed research; E.K.L., E.H.J., K.-A.S., B.C., M.K., and M.-S.K. performed research; K.-A.S., B.C., M.K., S.-H.K., S.J.K., and M.-S.K. contributed new reagents/analytic tools; E.K.L., E.H.J., K.-A.S., B.C., S.-H.K., and M.-S.K. analyzed data; and E.K.L., E.H.J., S.-H.K., and M.-S.K. wrote the paper.

The authors declare no conflict of interest.

This article is a PNAS Direct Submission.

[1]E.K.L., E.H.J., and K.-A.S contributed equally to this work.

[2]To whom correspondence may be addressed. Email: kmhyj.kim@samsung.com or mkang@skku.edu.

This article contains supporting information online at www.pnas.org/lookup/suppl/doi:10.1073/pnas.1407075112/-/DCSupplemental.

MICROBIOLOGY

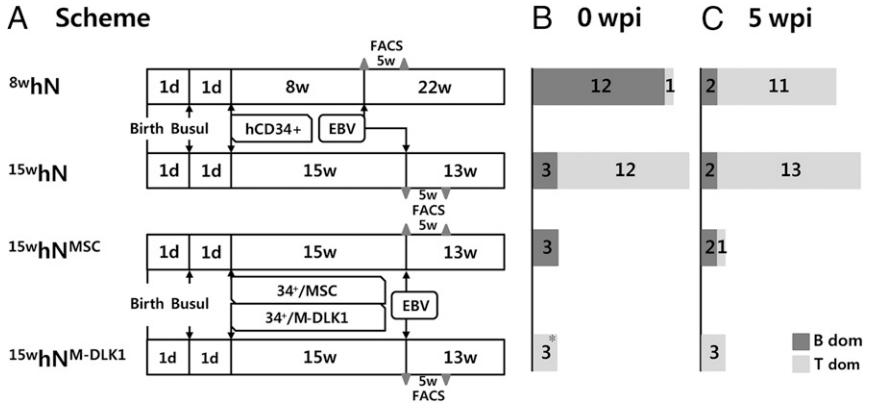

Fig. 1. Experimental schemes. (*A*) Four experimental settings were used to establish humanized mice and EBV infection. In the first and second trials, newborn mice (<1 d old) were injected i.p. with busulfan for bone marrow ablation, then 24 h later intrahepatically transplanted with 2×10^5 human cord blood CD34$^+$ HSCs. The mice were housed for 8 wk or 15 wk for reconstitution, then infected with EBV B95.8 virus or PBS through the tail vein. The mice were examined at 5 wpi by flow cytometry immune cell profiling (gray triangle), and housed for the indicated time or until moribund. In the third trial, the protocol for the second trial was followed, except that HSCs were engrafted along with nonautologous MSCs or MSCs expressing *DLK1*. ^{8w}hN denotes an hNSG (N) mouse reconstituted for 8 wk (8w) with hCD34$^+$ cells. (*B* and *C*) The number of mice with a predominance of B or T cells in PBMCs in experimental settings at 0 wpi (*B*) and 5 wpi (*C*). Note that four ^{8w}hN mice and five ^{15w}hN mice remained EBV-noninfection control in Cl (Table 1 and *SI Appendix*, Table S1). The fractions of hCD45 in PBMCs, CD45$^+$-gated CD19 cells, and CD45$^+$-gated CD3 cells were determined by flow cytometry.

evaluated (Fig. 1*A*). The 13 ^{8w}hN mice had an average of 6.6% hCD45 human leukocytes in peripheral blood mononuclear cells (PBMCs), among which a remarkably high percentage of hCD19$^+$ B cells (77.9%) and low percentage of hCD3$^+$ T-cells (4.9%) were repopulated (Fig. 2*A*). Individually, 12 of the 13 ^{8w}hN mice had predominant hCD19$^+$ B cells (Fig. 1).

At 8 wk plus 1 d postgrafting, these 13 mice were infected with EBV ($n = 9$ mice) or PBS ($n = 4$) and further evaluated for immune cell profiles at 5 and 22 wk postinfection (wpi). Consistent with earlier reports (18, 21), in 11 out of 12 ^{8w}hN mice, the number of hCD19 cells decreased sharply starting from 5 wpi and continuing until 22 wpi, whereas number of hCD3 cells increased at 5 wpi and then decreased thereafter up to 22 wpi (Figs. 1 *B* and *C* and 2*A*, and *SI Appendix*, Fig. S1). After EBV infection, eight of nine ^{8w}hN-EBV mice that exhibited B-cell predominance at the time of infection developed NHL type B-cell lymphomas. These NHLs were characterized by BCL2$^+$, hCD20$^+$, hKi67$^+$, EBNA1$^+$, EBNA2$^-$, and hCD30$^-$ cells. Seven of the eight mice showed no LMP1 expression (i.e., type I latency, EBNA2$^-$/LMP1$^-$) on immunohistochemical (IHC) analysis, and the remaining mouse showed LMP1 expression (i.e., type IIa latency, EBNA2$^-$ /LMP1$^+$) (*SI Appendix*, Fig. S2). None of the four noninfected mice (^{8w}hN-PBS) had a similar neoplasm (Table 1 and *SI Appendix*, Table S1).

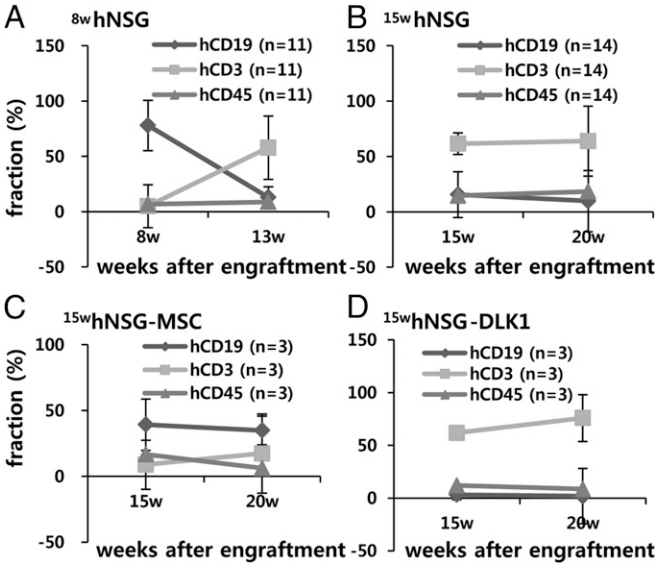

Fig. 2. Profiles of reconstituted human immune cells in PBMCs in humanized mice. (*A*) hCD45, hCD45-gated hCD19 (hCD19^{hCD45+}), and hCD3^{hCD45+} fractions in the 8-wk reconstitution group (^{8w}hN). (*B*) The 15-wk reconstitution group (^{15w}hN). (*C*) ^{15w}hNSG mice coimplanted with MSCs (^{15}hN^{MSC}). (*D*) ^{15w}hN mice coimplanted with MSCs expressing *DLK1* (^{15w}hN$^{M\text{-}DLK1}$). Data are mean ± SEM.

HL-Like Disorder in T-Cell–Predominant ^{15w}hN-EBV Mice. To establish humanized mice with T-cell dominance, NSG mice were housed for 15 wk after hCD34$^+$ HSC grafting (denoted by ^{15w}hN) (Fig. 1). This was done because the B-cell fraction decreased and the hCD3$^+$ fraction increased concurrently up to at least 13 wk after transplantation in this study (Fig. 2*A*) as well as previous studies (18, 21). In this study, the 15-wk reconstitution period resulted in a better-balanced repopulation overall. The ^{15w}hN mice ($n = 15$) had an average of 14.5% hCD45 cells, of which 61.4% were hCD3$^+$ T cells and only 15.5% were hCD19$^+$ B cells (Fig. 2*B*). Twelve of the 15 ^{15w}hN mice were T-cell predominant, whereas three remained B-cell predominant (Fig. 1*B*).

The mice were subjected to injection with PBS ($n = 5$) or EBV ($n = 10$). T-cell dominance remained unchanged in all 12 T-cell–predominant mice, and B-cell dominance was maintained in two of three mice. After EBV infection, 7 of 10 ^{15w}hN-EBV mice developed B-cell lymphomas, including NHL only in two mice, HL only in three mice, and both HL and NHL in two mice. None of the five noninfected mice (^{15w}hN-PBS) had such a neoplasm. EBV infection and infection-initiated virus release into mouse serum were confirmed by real-time quantitative PCR (qPCR), Epstein–Barr early DNA (EBER) in situ hybridization, and EBNA1 IHC staining. Substantially more hCD20$^+$ B cells and fewer hCD3$^+$ T cells were noted in splenic follicles. EBV DNA was detected earlier and diminished more quickly in the sera of mice with HL compared with mice with NHL (Fig. 3). More frequent splenomegaly was observed in infected mice (Fig. 3).

HL in EBV-Infected Humanized Mice Skewed with T-Cell Development. Our findings of HL-like tumor development in T-cell–predominant mice are consistent with the fact that T cells are associated predominantly with classical HL (25). We next attempted to establish humanized mice skewed with B or T cells to directly demonstrate the role of T-cell predominance in HL development. For this, six NSG mice were engrafted with hCD34$^+$ HSCs and nonautologous fetal liver (FL)-derived human mesenchymal stem cells (MSCs) expressing either vector or Notch ligand Delta-like-1 (DLK1) (Fig. 1 and *SI Appendix*). The mice were allowed 15 wk for reconstitution. This experimental design was based on the fact that expression of the Notch activator DKL1 is capable of skewing

Table 1. Summary of EBV-infected humanized mice

	EBV-noninfected in		EBV-infected in		
Phenotype*	B cells (n = 4)[†]	T cells (n = 5)[‡]	B cells (n = 14)	T cells (n = 11)	P value[§]
NHL	0	0	11	4[¶]	.0013
HL-like	0	0	0	8[¶]	
None[#]	4	5	3	2	NA
Evolution[‖]	T(4)	T (5**)	B (5**, [††], [‡‡]) T (9[§§])	T (11[¶¶])	NA

NA, not applicable.
*NHL, EBV-associated non-Hodgkin's-like lymphomas (EBV$^+$ BL, DLBCL, FBCL, and unspecified B-cell lymphoma), HL-like, EBV-associated Hodgkin's lymphoma (HL), or HL-like [HRS cells with hCD30$^+$/EBNA1$^+$ (EBER$^+$), hCD15$^+$].
[†]B-cell predominant mice with T-cell development suppressed at the time of EBV infection.
[‡]T-cell predominant mice with B-cell development suppressed at the time of EBV infection.
[§]Two-sided Fisher's exact t test.
[¶]Three mice showing both HL and NHL were included.
[#]No specific neoplasm.
[‖]Evolution of immune cell dominance by T or B cells for 5 wk after EBV infection or PBS (*SI Appendix*, Table S1 and Fig. 1).
**Presumed dominance in one mouse included.
[††]B-cell predominance was maintained in 5 of 14 infected mice, likely owing to EBV-mediated B-cell proliferation.
[‡‡]Three of five mice maintaining B-cell predominance developed NHL.
[§§]Eight of nine mice converted to T-cell predominance developed NHL.
[¶¶]T-cell predominance remained unchanged in all 11 mice.

HSCs to develop preferentially into T cells, whereas MSCs alone skew HSCs to develop preferentially into B cells (26, 27).

On evaluation, although the MSC and MSC-DLK1 methods reconstituted the total leukocyte population with comparable efficiency (hCD45$^+$, 16.73% vs. 11.9%) (Fig. 2 *C* and *D* and *SI Appendix*, Fig. S1), the three MSC-engrafted humanized mice displayed B-cell dominance (average, hCD19$^+$, 39.3% vs. hCD3$^+$, 8.9%) over T cells in PBMCs (Fig. 2*C* and Table 1). Two of the three B-cell–predominant mice developed NHL. In contrast, all three MSC-DLK1–engrafted humanized mice displayed T-cell dominance (average, hCD3$^+$, 61.8% vs. hCD19$^+$, 3.3%) over B cells, which persisted for the next 5 wk after engraftment (Figs. 1*B* and 2*D*). As a result, all three T-cell–predominant mice developed HL (Table 1 and *SI Appendix*, Figs. S3 and S4).

Taken together, the results of the three independent experimental trials suggest that B-cell predominance before EBV infection may have predisposed to NHL, whereas T-cell predominance was associated with, but not a prerequisite for, HL (P = 0.0013, Fisher's exact test). In other words, NHL more frequently (but not exclusively) developed in B-cell–predominant mice, and all cases of HL were developed in mice with T-cell predominance at the time of EBV infection. Immune cell evolution appeared to not be associated with phenotypic neoplasm (*SI Appendix*, Table S1).

Characteristics of Experimental EBV-Associated Lymphoma. Of note, after EBV infection, although eight of the nine ^{8w}hN mice had NHL, the 13 ^{15w}hN mice with mostly T-cell predominance before EBV infection developed HL-like tumors (n = 5), NHL (n = 4), or both NHL and H-like tumors (n = 3), indicating that T-cell predominance does not necessarily lead to the development of HL-like tumors (Table 1 and *SI Appendix*, Table S1 and Figs. S3–S5). HL-like splenocytes showed mostly type II latency (LMP1$^+$ and EBNA2$^-$ by IHC).

In neoplasms of T-cell–predominant ^{15w}hN-EBV mice, atypical, transformed large HRS cells surrounded by abundant nonmalignant lymphocytes were consistently encountered (average 24

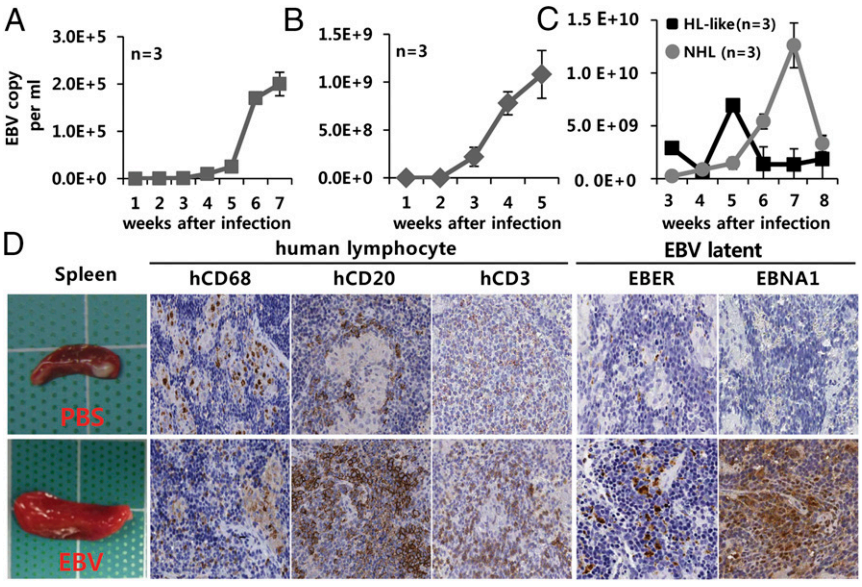

Fig. 3. Active secretion of EBV particles into sera and infection-induced lymphoproliferation. (*A*–*C*) Increased EBV copy number in serum from ^{8w}hN-EBV mice in the first experimental setting (*A*) and ^{15w}hN-EBV mice in the second setting (*B*), and copy number comparison between NHL and HL-like tumors in the second and third settings (*C*). Points represent average copy number ± SEM (n = 3) determined by qPCR for EBNA1. (*D*) Gross spleen morphology and in situ staining of ^{8w}hNSG spleen with human histiocyte marker hCD68, B-cell marker hCD20, T-cell marker hCD3, and latent EBV infection markers EBER and EBNA1. Similar staining patterns were observed in ^{15w}hN mice (*SI Appendix*, Fig. S12). (Scale bar: 100 μm.) Data are mean ± SEM.

HRS cells per spleen). Most of these transformed cells were consistent with EBV-associated HL-like phenotypes (e.g., hCD30$^+$, hCD15$^+$, hCD20$^{+/-}$, IgJ$^-$, hCD30$^+$/EBNA1$^+$, hCD30$^+$/EBER1$^+$, LMP1$^+$, EBNA2$^-$, phospho-STAT6$^+$), but were negative for the NHL markers hBCL2$^-$ in the hCD20$^{-/weak}$ background cells (Figs. 3 and 4*B* and *SI Appendix*, Figs. S3–S13). In H&E and immunophenotyping analyses, each spleen best diagnosed as HL-like had phenotypic hallmarks of HL based on updated Revised European–American Lymphoma (REAL)/World Health Organization (WHO) criteria (28): numerous atypical malignant EBV-positive HRS-like cells, lacunar-type HRS cells, and mummified HRS cells in association with predominant T cells or hCD68$^+$ histiocytes (29) (*SI Appendix*, Figs. S3 and S4). In addition, in accordance with the fact that STAT6 is constitutively phosphorylated in >80% of HRS cells of classical HL (30), phosphor-STAT6 was positive in all four HL-like tumors tested but negative in all three NHL tumors tested (*SI Appendix*, Fig. S12), supporting a diagnosis of HL-like tumors in this humanized setting. This activated the STAT6 signaling pathway, which most likely was activated by the cytokines IL-4 and IL-13, could induce EBV LMP1 even in the absence of EBNA-2, implicating type II EBV latent gene expression in EBVaHL (31) (*SI Appendix*, Fig. S3).

Costaining revealed colocalization of EBNA1 with hCD30 in HL-like cells. The lack of IHC-validated non-mouse hCD15 antibody for double IHC (note that EBNA1 Ab for IHC was a mouse monoclonal Ab) hindered the double staining in HRS cells. Instead, additional EBER and hCD30 double staining further demonstrated EBER$^+$/hCD30$^+$ colocalization in HRS-like cells (Fig. 4*B* and *SI Appendix*, Fig. S3). EBNA1 was costained with hCD20 in B-cell–high NHL tissue (Fig. 4), which was supported by an abundance of hCD20$^+$ cells in NHL. In contrast, EBNA1$^+$ HRS cells were mostly negative for hCD20 (*SI Appendix*, Figs. S3 and S6), which is also consistent with the fact that HL cells are hCD20$^{-/+}$ based on the REAL/WHO criteria. Numerous human hCD20$^+$ cells were present in uninfected spleen. In support of these data, EBNA1 was clearly negative in these uninfected cells by qPCR (*SI Appendix*, Figs. S6 and S13). qPCR revealed hCD30 expression in HL-like tissues, but not in NHL or uninfected spleen (*SI Appendix*, Fig. S13). In addition, there were frequent somatic hypermutations (SHMs) in cDNA encoding the Ig heavy-chain variable region (V_H) of spleen DNA of HL-like and NHL tumors from EBV-infected humanized mice (*SI Appendix*, Fig. S14). In contrast, B-cell–predominant mice from the ^{8w}hN-EBV group exhibited EBVaNHL-like neoplasms (e.g., DLBCL, BL) that showed extensive or complete distortion of splenic architecture with malignant immature lymphoproliferation. In keeping with the criteria for NHL (e.g., hBCL2$^+$, hCD20$^{+/hi}$) (28), these cancerous lesions were consistently positive for EBV-associated NHL markers (hCD20$^+$, hBCL2$^+$, hKi67$^+$, EBER$^+$, EBNA1$^+$, and hCD20$^+$/EBNA1$^+$) but mostly negative for type II/III latency markers (EBNA2$^-$ and LMP1$^-$) and HL markers (hCD30$^-$ and hCD15$^-$) (Fig. 4*A* and SI *Appendix*, Figs. S2 and S6–S12). These data suggest that infection of ^{8w}hN with EBV results in NHL-type neoplasms with predominant type I latent infection. Analytical qPCR analyses for spleen cDNA confirmed the result of type I latency in the ^{8w}hN-EBV mice (*SI Appendix*, Fig. S13).

Discussion

In the present study, humanized mice recapitulated many of key characteristics of EBV infection-associated disease pathogenesis. EBV-associated disorders in humanized mice, including post-transplantation lymphoproliferative disorder, NHL (DLBCL, FBCL), HLH, arthritis, and chronic active EBV infection, have been reproduced. The outcome should depend on different inputs (e.g., strain, age of recipient, donor cells, duration of

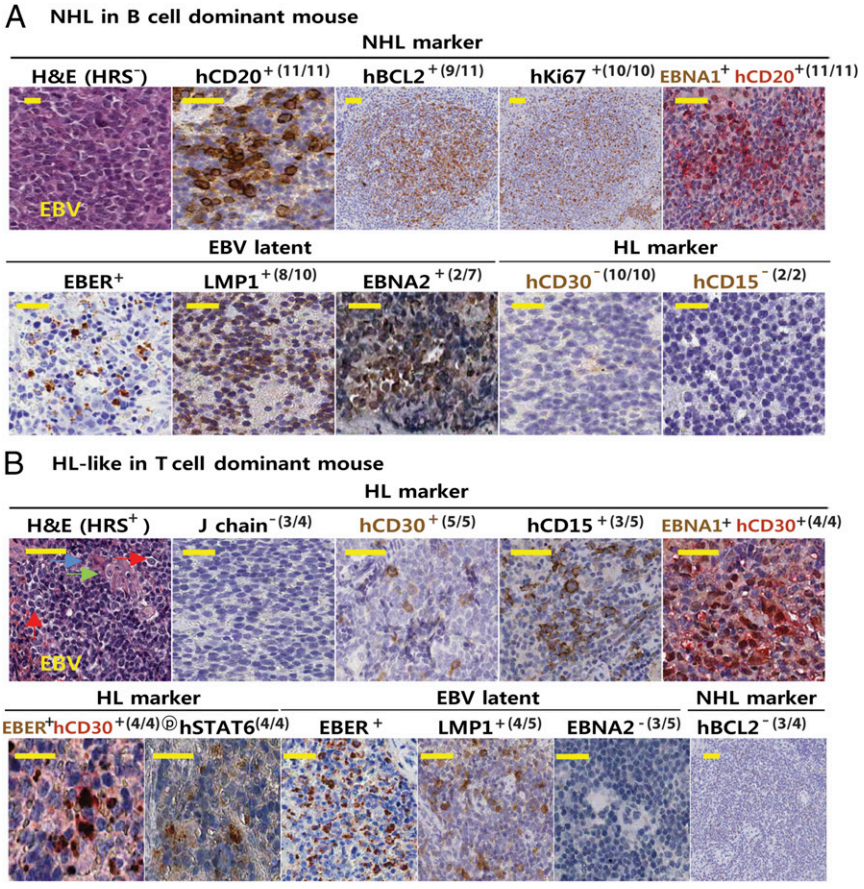

Fig. 4. Immunophenotypes of tumor-bearing spleens. (*A*) H&E and IHC staining of spleens bearing EBV-associated NHL tumors (hN-EBV-NHL; n = 10) among EBV-infected B-cell–predominant mice (hN-EBV; n = 11). Results are presented with NHL (e.g., DLBCL)-inclusive markers (hCD20$^+$, hBCL2$^+$, and Ki67$^+$), type I EBV latency markers (EBER$^+$, EBNA1$^+$, LMP1$^{-8/10\ tested}$, and EBNA2$^{-5/7}$) and DLBCL-exclusive markers (hCD30$^-$ and hCD15$^-$). Note the negative staining of these NHL tissues with the NHL-exclusive marker phospho-STAT6$^{-4/4}$, as shown in *SI Appendix*, Fig. S12. (*B*) H&E and IHC staining patterns of spleens bearing EBV-associated HL-like tumors (hN-EBV-HL-like; n = 5) among EBV-infected T-cell–predominant mice (hN-EBV; n = 8). Results are presented with EBVaHL-inclusive markers (hCD20$^{-/weak}$, hCD15$^+$, hCD30$^+$, IgJ chain$^-$, EBER$^+$/hCD30$^+$, EBNA1$^+$/hCD30$^+$, EBER$^+$, EBNA1$^+$, LMP1$^{+4/5}$, EBNA2$^{-3/5}$, and phospho-STAT6$^{+4/4}$) and HL-exclusive markers (hBCL2$^-$ and hCD45$^-$). Numerous typical binucleated HRS (red arrow) or lacunar RS-like cells (green arrow) and mummified RS cells (blue arrow) per spleen were observed in HL-like tumors. The binucleated RS nucleus contains a prominent eosinophilic nucleolus with perinucleolar halos, giving the cell an "owl's eye" appearance. Note the coexpression of hCD30 and EBNA1 (or EBER) in HRS-like cells of HL-like tumors (*SI Appendix*, Figs. S3 and S5).

reconstitution, dose of EBV, depth of analyses) (16–18, 20–23). IHC staining of spleen sections for EBV latent gene markers identified EBV infection in these humanized mice (*SI Appendix*, Figs. S8–S11). To our knowledge, this study is the first to describe EBVaHL-like disorder in multiple humanized mice with supportive evidence. The malignant HL-like tissues in this study were characterized by atypical EBV-infected HRS or HRS-like cells. Similar to typical HRS, where 90% HRS of human HL tissues in situ is $hCD20^{-/weak}$, the HL-like tissues in this study were clearly $hCD20^{-/weak}$, also consistent with the updated REAL/WHO criteria (28) and thus strongly suggestive of experimental HL-like neoplasms (12–14, 28, 32, 33). T-cell preexpansion likely does not prevent EBV lymphomagenesis, because T-cell–dominant mice developed lymphoma; rather, preconditioned mice with B-cell predominance (or T-cell suppression) developed NHL after EBV infection (Table 1 and *SI Appendix*, Table S1). Most of the NHL neoplasms in this study were characterized by $hBCL2^+$, $hKI67^+$, $hCD30^-$, $EBER^+$, $EBNA2^-$, and LMP^- expression. Three mice were found to have both NHL and HL-like tumors.

Watanabe et al. (34) previously reported that a significant number of B-cell progenitors accumulate in the spleen in human cord blood-derived $hCD34^+$ HSC-reconstituted humanized NSG (or NOG) mice. Numerous other groups also have reported obvious immature B-cell predominance in the periphery and spleen, especially in humanized mice reconstituted for short periods (<12 wk) (18, 34–38). Therefore, the predominant B cells before EBV infection in the ^{8w}hN mice in this study are believed to be immature B cells, which will differentiate to develop mature B-cell and T-cell fractions. In this regard, the development of NHL primarily in the ^{8w}hN mice after EBV infection (^{8w}hN-EBV; eight of nine mice) suggests that a significant fraction of immature B cells at the time of EBV infection are likely associated with NHL development, although our study does not provide direct evidence of this. Despite apparent normal T-cell development, $hCD3^+$ T cells could have functional abnormalities in central or peripheral lymphoid organs (34), related mainly to the lack of human thymic tissues normally required for thymic education during functional T-cell development. Inappropriate or incomplete immune function should affect malignant transformation after EBV infection. Nevertheless, many of the HL-like tumors in these mice displayed multiple HRS and lacunar-type cells with broken spleen architecture, the usual lack of germinal center, frequent—but not always (or entire)—loss of lymphoid follicles (LFs) or LFs replaced with immature cells, frequent enlargement of white pulp or periarteriolar lymphoid sheaths (PALS), and often atrophy in red pulp. Therefore, the malignant HL-like tumor cells in this study were defined as atypical giant cells within or near abundant immature lymphocytes that replace follicles or disrupt splenic normal architecture such as follicles and germinal centers. Besides coexisting NHL or infectious mononucleosis (IM) in certain mice, almost all of the tumors in T-cell–dominant conditioned mice in this study certainly contained subsets of HL-like tumors, because they displayed multiple criteria of HL (i.e., frequent HRS cells with $J\ chain^-$, $CD30^+$, $CD15^+$, $EBER^+$, $EBNA2^-$, $hBCl2^-$, and phospho-$STAT6^+$) (*SI Appendix*, Fig. S12) (30). The activated STAT6 signaling pathway could induce EBV LMP1 in absence of EBNA-2, implicating type II EBV latent gene expression in EBVaHL (30, 31). The majority of HL-like tumors exhibited type 2 latency; five of eight HL-like tumors displayed type 2a latency ($LMP1^+/EBNA2^-$), whereas the remaining three showed apparent type 3 latency. Despite having multiple molecular characteristics of HL, the apparent type 3 latency in these three so-called "HL-like" tumors is not typically observed in human HL. This is suggestive of an atypical HL that may occur in certain conditions, such as an experimental animal model. On the other hand, given that the "markers" (such as CD30) used to define HL are not absolutely specific for HL, and that the EBV latency type is not that seen in human HL, it also is possible that the tumors in this T-cell–predominant model may be atypical HL-like tumors rather than true representatives of HL.

Because patients with a history of IM have a threefold to fourfold increased risk of developing HL (39–41) and IM may exhibit occasional HRS-like cells with $CD30^+$, $LMP1^+$, and $EBNA2^+$ (42), HRS-like cells can be observed in EBV-infected humanized mice. Therefore, we carefully readdressed the issue. In addition to more abundant HRS-like cells in HL-like tissues, we observed IM-like cells, albeit infrequently (*SI Appendix*, Fig. S5*C*). However, the rare IM-like cells were monocytes resembling atypical lymphocytes (reactive immunoblasts of the germinal center) and had different microenvironments than those of HRS cells. In the rare IM-like lesions found in this study, the basic microstructure of the lymphoid tissue was preserved, including the lymphoid follicles and PALS. In accordance with the fact that IM is an inflammatory and reactive condition in which basic lymphoid tissue can usually be restored after the termination of infection, we observed mixed populations of immunoblasts, lymphocytes, and various kinds of inflammatory cells in response to EBV infection in IM lesions (*SI Appendix*, Fig. 5*C*), supporting their infrequent presence.

Given that IM has no evidence of crippling SHMs in the V_H gene (43), whereas HL has nonsense or deletion mutation in the V_H gene, resulting in loss of the correct reading frame in ∼30% of cases (44), the presence of SHMs in the HL-like tumors in this study further supports a pathological diagnosis of HL-like malignancy. SMHs were identified in all tumors examined, regardless of the presence of IM-like lesions. This is because malignant cells were present in all tissues examined. In addition to $hCD30^+/hCD15^+/EBNA1^+/EBER^+$, the presence of phosphor-$STA6^+$ HRS-like cells and a V_H nonsense mutation strengthened the diagnosis of EBVaHL-like tumors (Fig. 4). The coexistence of occasional type III IM cells and type II HL-like cells accounts for the apparent type III latency in some of the HL-like tumor-bearing spleens. Along with the coexisting NHL or IM, almost all tumors in the T-cell–dominant conditioned mice in this study also contained subsets of HL-like tumors. Of note, the results showing apparently fewer numbers of EBER-positive cells than EBNA1-positive cells shown in Figs. 3 and 4 and *SI Appendix*, Figs. S8 and S9 were confirmed by additional staining (*SI Appendix*, Fig. S15). The discrepancy is likely due to decreased EBER promoter activity by unphosphorylated active retinoblastoma tumor-suppressor protein during cell cycle phases G(0) and early G(1) (45, 46).

Materials and Methods

Ethics Statement. Human protocol (IRB file no. 2010-08-159) for human material was approved by the Institutional Review Boards of Samsung Medical Center. Animal protocol (no. 20100210001) was approved by the Institutional Animal Care and Use Committee (IACUC) of Samsung Biomedical Research Institute (SBRI) (see *SI Appendix* for detail). Cell preparation for engraftment, infection with EBV, and characterization of humanized NSG (hNSG) mice are described in detail in *SI Appendix*.

Preparation of Humanized Mice. Nonobese diabetic/severe combined immunodeficient mice with IL2R knockout (NOD/LtSz-*scid*/*IL2R*γ^{null}), referred to herein as NSG, were purchased from The Jackson Laboratory (47, 48). Newborn progenies for transplantation experiments were obtained from inbred breeding and maintained under specific pathogen-free conditions. For reconstitution of the HIS in mice, 1-d-old newborn female NSG mice were injected i.p. with busulfan (Ben Benue Laboratories) at a dose of 15 mg/kg to ablate residual bone marrow (47, 48). At 24 h after busulfan injection, 2×10^5 $hCD34^+$ HSCs were injected intrahepatically.

The mice were housed for 8 or 15 wk before characterization and EBV infection (Fig. 1*A*). NSG mice reconstituted with HIS components are referred to as hNSG mice. Reconstitution was evaluated as described previously (20, 24). Where necessary, humanized mice with skewed populations of B or T cells were generated as described above with the following modifications. B-cell–predominant NSG mice were coengrafted with cord blood $hCD34^+$ HSCs and human FL-MSCs, which enhanced HSC engraftment and suppressed T-cell proliferation (49–52). This treatment resulted in B-cell–predominant humanized

MICROBIOLOGY

mice. T-cell–predominant NSG mice were coengrafted with cord blood hCD34$^+$ HSCs and hFL-MSC-DLK1 cells expressing an activated Notch ligand (DLK1) to suppress B-cell development (53). This treatment resulted in T-cell–predominant humanized mice. After 15 wk, mice were infected with EBV as described in *SI Appendix*, followed by investigation for 13 wk.

ACKNOWLEDGMENTS. We thank Professor Young-Hyeh Ko at Samsung Medical Center, a board member of the Korean Society of Hematologic Pathology, for helpful comments. This study was supported by Grants SMX1132731, SMX1132461, and OB00013 from the Samsung Biomedical Research Institute and Samsung Medical Center; Grants HI09C1552, A110637 (to E.K.L.), and HI13C1263 from the Korea Health Technology Research and Development (R&D) Project through the Korea Health Industry Development Institute, funded by the Ministry for Health & Welfare, Republic of Korea; Grant 1120010 from the National R&D Program for Cancer Control, Ministry for Health and Welfare, Republic of Korea; and Grant 2011-0012393 from the Basic Science Research Program through the National Research Foundation of Korea, funded by the Ministry of Education, Science and Technology.

1. Epstein MA, Achong BG, Barr YM (1964) Virus particles in cultured lymphoblasts from Burkitt's lymphoma. *Lancet* 1(7335):702–703.
2. Epstein MA, Barr YM (1964) Cultivation in vitro of human lymphoblasts from Burkitt's malignant lymphoma. *Lancet* 1(7327):252–253.
3. Kieff ED, Rickinson AB (2007) Epstein-Barr virus and its replication. *Fields Virology*, eds Knipe DM, Howley PM (Lippincott Williams & Wilkins, Philadelphia), 5th Ed, Vol 2, pp 2603–2654.
4. Küppers R, Engert A, Hansmann ML (2012) Hodgkin lymphoma. *J Clin Invest* 122(10): 3439–3447.
5. Glaser SL, et al. (1997) Epstein-Barr virus-associated Hodgkin's disease: Epidemiologic characteristics in international data. *Int J Cancer* 70(4):375–382.
6. Jarrett RF, et al.; Scotland and Newcastle Epidemiology of Hodgkin Disease Study Group (2005) Impact of tumor Epstein-Barr virus status on presenting features and outcome in age-defined subgroups of patients with classic Hodgkin lymphoma: A population-based study. *Blood* 106(7):2444–2451.
7. Zhang Y, et al. (2010) The prevalence of Epstein-Barr virus infection in different types and sites of lymphomas. *Jpn J Infect Dis* 63(2):132–135.
8. Zhou XG, Hamilton-Dutoit SJ, Yan QH, Pallesen G (1993) The association between Epstein-Barr virus and Chinese Hodgkin's disease. *Int J Cancer* 55(3):359–363.
9. Weiss LM, Movahed LA, Warnke RA, Sklar J (1989) Detection of Epstein-Barr viral genomes in Reed-Sternberg cells of Hodgkin's disease. *N Engl J Med* 320(8):502–506.
10. Khan G, Coates PJ, Gupta RK, Kangro HO, Slavin G (1992) Presence of Epstein-Barr virus in Hodgkin's disease is not exclusive to Reed-Sternberg cells. *Am J Pathol* 140(4): 757–762.
11. Kapatai G, Murray P (2007) Contribution of the Epstein-Barr virus to the molecular pathogenesis of Hodgkin lymphoma. *J Clin Pathol* 60(12):1342–1349.
12. Jarrett RF (2006) Viruses and lymphoma/leukaemia. *J Pathol* 208(2):176–186.
13. Pallesen G, Hamilton-Dutoit SJ, Rowe M, Young LS (1991) Expression of Epstein-Barr virus latent gene products in tumour cells of Hodgkin's disease. *Lancet* 337(8737): 320–322.
14. Herbst H, et al. (1991) Epstein-Barr virus latent membrane protein expression in Hodgkin and Reed-Sternberg cells. *Proc Natl Acad Sci USA* 88(11):4766–4770.
15. Izumi KM, et al. (1999) The Epstein-Barr virus oncoprotein latent membrane protein 1 engages the tumor necrosis factor receptor-associated proteins TRADD and receptor-interacting protein (RIP) but does not induce apoptosis or require RIP for NF-kappaB activation. *Mol Cell Biol* 19(8):5759–5767.
16. Sato K, et al. (2011) A novel animal model of Epstein-Barr virus-associated hemophagocytic lymphohistiocytosis in humanized mice. *Blood* 117(21):5663–5673.
17. White RE, et al. (2012) EBNA3B-deficient EBV promotes B cell lymphomagenesis in humanized mice and is found in human tumors. *J Clin Invest* 122(4):1487–1502.
18. Yajima M, et al. (2008) A new humanized mouse model of Epstein-Barr virus infection that reproduces persistent infection, lymphoproliferative disorder, and cell-mediated and humoral immune responses. *J Infect Dis* 198(5):673–682.
19. Yajima M, et al. (2009) T cell-mediated control of Epstein-Barr virus infection in humanized mice. *J Infect Dis* 200(10):1611–1615.
20. Ma SD, et al. (2011) A new model of Epstein-Barr virus infection reveals an important role for early lytic viral protein expression in the development of lymphomas. *J Virol* 85(1):165–177.
21. Ma SD, et al. (2012) An Epstein-Barr Virus (EBV) mutant with enhanced BZLF1 expression causes lymphomas with abortive lytic EBV infection in a humanized mouse model. *J Virol* 86(15):7976–7987.
22. Imadome K, et al. (2011) Novel mouse xenograft models reveal a critical role of CD4$^+$ T cells in the proliferation of EBV-infected T and NK cells. *PLoS Pathog* 7(10): e1002326.
23. Kuwana Y, et al. (2011) Epstein-Barr virus induces erosive arthritis in humanized mice. *PLoS One* 6(10):e26630.
24. Islas-Ohlmayer M, et al. (2004) Experimental infection of NOD/SCID mice reconstituted with human CD34$^+$ cells with Epstein-Barr virus. *J Virol* 78(24):13891–13900.
25. Atayar C, et al. (2007) Hodgkin's lymphoma associated T-cells exhibit a transcription factor profile consistent with distinct lymphoid compartments. *J Clin Pathol* 60(10): 1092–1097.
26. Abdallah BM, et al. (2007) dlk1/FA1 regulates the function of human bone marrow mesenchymal stem cells by modulating gene expression of pro-inflammatory cytokines and immune response-related factors. *J Biol Chem* 282(10):7339–7351.
27. Schmitt TM, Zúñiga-Pflücker JC (2002) Induction of T cell development from hematopoietic progenitor cells by delta-like-1 in vitro. *Immunity* 17(6):749–756.
28. Hoffbrand AV, Pettit JE, Vya P (2010) Hodgkin's lymphoma. *Color Atlas of Clinical Hematology*, eds Hoffbrand AV, Pettit JE, Vya P (Mosby Elsevier Science, Philadelphia), Vol 1, pp 379–392.
29. Mani H, Jaffe ES (2009) Hodgkin lymphoma: An update on its biology with new insights into classification. *Clin Lymphoma Myeloma* 9(3):206–216.
30. Skinnider BF, et al. (2002) Signal transducer and activator of transcription 6 is frequently activated in Hodgkin and Reed-Sternberg cells of Hodgkin lymphoma. *Blood* 99(2):618–626.
31. Kis LL, et al. (2011) STAT6 signaling pathway activated by the cytokines IL-4 and IL-13 induces expression of the Epstein-Barr virus-encoded protein LMP-1 in absence of EBNA-2: implications for the type II EBV latent gene expression in Hodgkin lymphoma. *Blood* 117(1):165–174.
32. Harris NL, et al. (1999) World Health Organization classification of neoplastic diseases of the hematopoietic and lymphoid tissues: Report of the Clinical Advisory Committee meeting, Airlie House, Virginia, November 1997. *J Clin Oncol* 10(12):1419–1432.
33. Küppers R, Yahalom J, Josting A (2006) Advances in biology, diagnostics, and treatment of Hodgkin's disease. *Biol Blood Marrow Transplant* 12(1, Suppl 1):66–76.
34. Watanabe Y, et al. (2009) The analysis of the functions of human B and T cells in humanized NOD/shi-scid/gammac(null) (NOG) mice (hu-HSC NOG mice). *Int Immunol* 21(7):843–858.
35. Lang J, et al. (2013) Studies of lymphocyte reconstitution in a humanized mouse model reveal a requirement of T cells for human B cell maturation. *J Immunol* 190(5): 2090–2101.
36. Vuyyuru R, Patton J, Manser T (2011) Human immune system mice: Current potential and limitations for translational research on human antibody responses. *Immunol Res* 51(2-3):257–266.
37. Biswas S, et al. (2011) Humoral immune responses in humanized BLT mice immunized with West Nile virus and HIV-1 envelope proteins are largely mediated via human CD5$^+$ B cells. *Immunology* 134(4):419–433.
38. Watanabe S, et al. (2007) Hematopoietic stem cell-engrafted NOD/SCID/IL2Rgamma null mice develop human lymphoid systems and induce long-lasting HIV-1 infection with specific humoral immune responses. *Blood* 109(1):212–218.
39. Muñoz N, Davidson RJ, Witthoff B, Ericsson JE, De-Thé G (1978) Infectious mononucleosis and Hodgkin's disease. *Int J Cancer* 22(1):10–13.
40. Hjalgrim H, et al. (2000) Risk of Hodgkin's disease and other cancers after infectious mononucleosis. *J Natl Cancer Inst* 92(18):1522–1528.
41. Hjalgrim H, et al. (2003) Characteristics of Hodgkin's lymphoma after infectious mononucleosis. *N Engl J Med* 349(14):1324–1332.
42. Pfreundschuh M, et al. (1990) Detection of a soluble form of the CD30 antigen in sera of patients with lymphoma, adult T-cell leukemia and infectious mononucleosis. *Int J Cancer* 45(5):869–874.
43. Kurth J, et al. (2000) EBV-infected B cells in infectious mononucleosis: Viral strategies for spreading in the B cell compartment and establishing latency. *Immunity* 13(4): 485–495.
44. Kanzler H, Küppers R, Hansmann ML, Rajewsky K (1996) Hodgkin and Reed-Sternberg cells in Hodgkin's disease represent the outgrowth of a dominant tumor clone derived from (crippled) germinal center B cells. *J Exp Med* 184(4):1495–1505.
45. Scott PH, et al. (2001) Regulation of RNA polymerase III transcription during cell cycle entry. *J Biol Chem* 276(2):1005–1014.
46. Larminie CG, et al. (1997) Mechanistic analysis of RNA polymerase III regulation by the retinoblastoma protein. *EMBO J* 16(8):2061–2071.
47. Ito M, et al. (2002) NOD/SCID/gamma(c)(null) mouse: An excellent recipient mouse model for engraftment of human cells. *Blood* 100(9):3175–3182.
48. Shultz LD, et al. (2005) Human lymphoid and myeloid cell development in NOD/LtSz-scid IL2R gamma null mice engrafted with mobilized human hemopoietic stem cells. *J Immunol* 174(10):6477–6489.
49. in 't Anker PS, et al. (2003) Mesenchymal stem cells in human second-trimester bone marrow, liver, lung, and spleen exhibit a similar immunophenotype but a heterogeneous multilineage differentiation potential. *Haematologica* 88(8):845–852.
50. Bartholomew A, et al. (2002) Mesenchymal stem cells suppress lymphocyte proliferation in vitro and prolong skin graft survival in vivo. *Exp Hematol* 30(1):42–48.
51. Di Nicola M, et al. (2002) Human bone marrow stromal cells suppress T-lymphocyte proliferation induced by cellular or nonspecific mitogenic stimuli. *Blood* 99(10): 3838–3843.
52. Tse WT, Pendleton JD, Beyer WM, Egalka MC, Guinan EC (2003) Suppression of allogeneic T-cell proliferation by human marrow stromal cells: Implications in transplantation. *Transplantation* 75(3):389–397.
53. Raghunandan R, et al. (2008) Dlk1 influences differentiation and function of B lymphocytes. *Stem Cells Dev* 17(3):495–507.